Journal of Applied Polymer Science

Ultrasound Assisted Continuous-Mixing for the Preparation of PP/SEBS/OMMT Ternary Nanocomposites

Ying Liu, Linsheng Xie, Yulu Ma, Haitao Liu, Haili Zhao, Yunxiang Wang
School of Mechanical and Power Engineering, East China University of Science and Technology, Shanghai, 200237, China
Correspondence to: Y. Ma (E-mail: myl@ecust.edu.cn)

ABSTRACT: Polypropylene (PP)/polystyrene-*block*-poly(ethylene-*co*-butylenes)-*block*-polystyrene (SEBS)/organo-montmorillonite (OMMT) nanocomposites of varying concentrations of maleic anhydride-grafted polypropylene (PP-*g*-MA) were prepared by continuous mixing assisted by ultrasonic oscillation. The structure and morphology of nanocomposites were investigated by X-ray diffraction (XRD), transmission electron microscopy, and scanning electron microscopy. It was found that both PP-*g*-MA and ultrasonic oscillation could enhance the intercalation and exfoliation of OMMT in PP matrix. Meanwhile, the formation of β-form PP could be induced by ultrasonic irradiation at a power of more than 540 W. Rheological properties including complex viscosity, storage, and loss modulus of nanocomposites were increased after adding PP-*g*-MA or ultrasonic treatment. The results of mechanical properties showed that PP-*g*-MA could improve the tensile strength and tensile modulus of nanocomposites, but with the sacrifice of impact strength. This problem could be improved by ultrasound due to the reduced particle size of SEBS. However, the mechanical properties would be reduced by ultrasonic treatment with higher intensity due to the polymer degradation. Therefore, the synergistic effect of both compatibilizer and ultrasound should account for the balance between toughness and stiffness of PP/SEBS/OMMT ternary nanocomposites. © 2014 Wiley Periodicals, Inc. J. Appl. Polym. Sci. **2014**, *131*, 41202.

KEYWORDS: continuous mixing; PP-*g*-MA; PP/SEBS/OMMT nanocomposites; ultrasound

Received 1 May 2014; accepted 22 June 2014
DOI: 10.1002/app.41202

INTRODUCTION

Polypropylene (PP) is one of the most widely used polyolefin polymers owing to its advantages such as low density, low price, high heat resistance, and good processability. However, the application of PP is still limited by its poor impact toughness, especially at low temperature and high impact rate.[1] To improve its impact strength, the addition of an elastomer is an effective way, whereas it usually lowers modulus.[1] To overcome this problem, the addition of a filler is an appropriate way for reinforcing PP. Therefore, a ternary composites consisting of PP matrix, elastomer and filler is considered to be an attractive material to obtain an balance of toughness and stiffness.[2–5] In recent years, great attentions had been paid to the PP/elastomer/clay nanocomposites due to their high levels of reinforcement obtained by low concentrations of nanoclays.[6–11] To enhance the compatiblility of nanoclay such as montmorillonite (MMT) with nonpolar PP chains, it is common to use the organically modified montmorillonite (OMMT) as the reinforcing filler and incorporate maleic anhydride grafted polypropylene (PP-*g*-MA) as a compatibilizer.

Several studies with regard to the preparation of PP/elastomer/clay nanocomposites were reported. Hejazi et al.[7] studied the mechanical properties of PP/EPDM/organoclay prepared with PP-*g*-MA by twin screw extrusion. They reported that the tensile strength and modulus of the blends increased with the incorporation of nanoclay and PP-*g*-MA. They also reported that a high degree of exfoliation of the organoclay layers by melt processing seems to require high shear rate and appropriate residence time. Tjong et al.[12] studied the structure-property relationship of PP/OMMT nanocomposites toughened with SEBS-*g*-MA, the results showed that a double impact strength was obtained when small amounts of OMMT (2%) were added in PP/20%SEBS-*g*-MA composite. Su and Huang[13] argued that the synergistic effect of SEBS and OMMT should be responsible for the balance of stiffness-toughness performance of PP/SEBS/OMMT ternary composites. Zina Vuluga et al.[14] investigated the effects of SEBS on mechanical and thermal properties of PP blended with and without nanoclay. They obtained the best stiffness-toughness balance in the case of PP/23%SEBS/10%OMMT, which resulted in a significant increase of elongation, energy at break and impact strength (13, 10, and 22 times of the case of PP/10%OMMT, respectively). However, all of these papers mainly aimed to investigate the effect of elastomer, nanoclay or compatibilizer contents on mechanical properties of PP nanocomposites and seek for a right balance between toughness

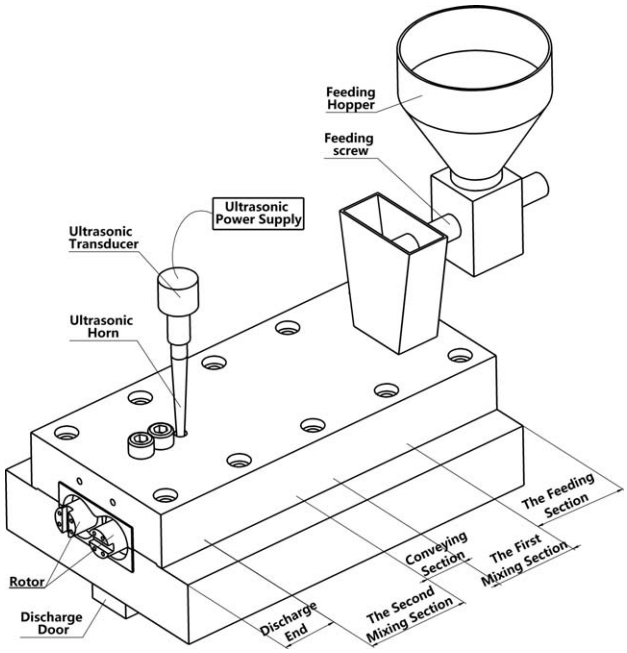

Figure 1. Schematic diagram of two-rotor continuous mixer with high-intensity ultrasonic system.

and stiffness provided by the incorporation of elastomer and clay, no report has been published regarding the mixing method that can enhance the dispersion of elastomer and nanoclay in PP matrix. It is worth noting that the properties of the ternary nanocomposites are determined not only by the components of the nanocomposites but also by the microstructure of composites, particularly the dispersion of nanoparticles in polymer matrix. However, common melt blending through extruder is usually less efficient when the reinforcing filler is in nanoscale.[15]

To enhance the dispersion, especially the nanoscale dispersion of particles in polymer matrix, a great number of studies on application of ultrasound in melt blending of polymer-based composites were reported in recent years.[15–22] They all found that the chemical and physical effects of the ultrasound could assist in better filler-dispersion and improve the *in situ* compatibility of immiscible blends. The compatibility was enhanced by the recombination of different macroradicals formed by chain scission of the polymer in the presence of ultrasound.

In this article, polystyrene-*block*-poly(ethylene-*co*-butylenes)-*block*-polystyrene (SEBS) was used as an elastomer. When it comes to the preparation of PP/SEBS/OMMT nanocomposites, the most attempts were by melt intercalation in twin screw extruder or intensive batch mixer,[1,12–14,23–25] no report has been published regarding the processing of the ternary nanocomposites using ultrasound-assisted mixing in two-rotor continuous mixer (FCM). Therefore, we try to obtain an uniform dispersion of OMMT and SEBS in PP matrix by continuous mixing in FCM with the aid of ultrasound. The effects of ultrasonic irradiation and compatibilizer (PP-*g*-MA) on structural properties, morphology, rheological, and mechanical properties of PP/SEBS/OMMT nanocomposites were studied.

EXPERIMENTAL

Material and Equipment

The matrix PP was homo-PP (MFI = 26 g/10 min@230°C/2.16 kg, Y2600T, Sinopec Shanghai Petrochemical, Shanghai, China). The elastomer (SEBS) used in this research was Kraton G1650 M from Kraton Polymers (USA), a linear poly[styrene-(ethylene-*co*-butylene)-styrene] block copolymer with a styrene content of 30%, density of 0.224 g/cm^3, and MFI < 1 g/10 min (230°C/5 kg). DK1N natural montmorillonite, modified with octadecylammonium, with a cation exchange capacity of 90 meq/100 g and *d*-spacing of 2.4 nm, was supplied by Zhejiang FengHong New Material. Maleic anhydride-grafted PP (PP-*g*-MA) was obtained from DuPont, Fusabond P353, with a MFI of 450 g/10 min (190°C/2.16 kg) and a density of 0.904 g/cm^3.

Table I. Compositions of the PP-Based Composites

Sample	PP (ph)	SEBS (ph)	O-MMT (ph)	PP-*g*-MA (ph)	Ultrasonic power (W)	Feeding rate (kg/h)
S1	100	0	0	0	0	3.5
S2	95	15	5	0	0	3.5
S3	95	15	5	5	0	3.5
S4	95	15	5	10	0	3.5
S5	95	15	5	15	0	3.5
S6	95	15	5	0	180	3.5
S7	95	15	5	0	540	3.5
S8	95	15	5	0	810	3.5
S9	95	15	5	5	810	3.5
S10	95	15	5	10	810	3.5
S11	95	15	5	15	810	3.5
S12	95	15	5	0	810	1.5
S13	95	15	5	0	810	2.5
S14	95	15	5	0	810	4.5
S15	95	15	5	0	810	5.5

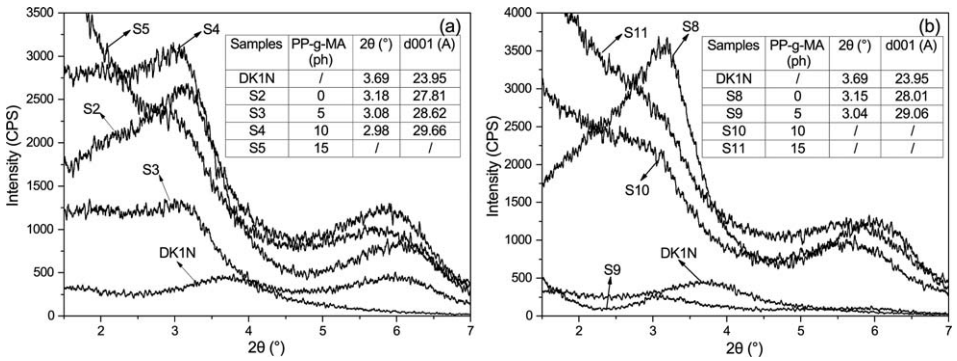

Figure 2. Small-angle XRD patterns of OMMT (DKIN) and PP nanocomposites at different compatibilizer loadings without (a) and with (b) ultrasonic treatment at an power of 810 W.

The ultrasound-mixing experimental equipment consists of a two-rotor continuous mixer (ECM30, 29 mm rotor diameter, $L/D = 9$, 3 mm gap size between the two rotors) and the ultrasonic supply (SM-900DY, Shunma, Nanjing, China) as shown in Figure 1. The mixer has two mixing sections, and the ultrasonic supply was added at the second mixing section, where all of the polymer had been melted. The ultrasonic frequency is 20 kHz and power ranges from 0 to 900 W. The ultrasonic horn (3 mm diameter at tip) was in direct contact with the polymer melt, providing the longitudinal vibrations in the direction perpendicular to the flow direction.

Preparation of Composites

According to the compositions shown in Table I, the PP blends were mixed prior to processing by three-dimensional efficient mixer for 15 min. The mixture was then dried for 5 h at 80°C in a vacuum oven. The temperature in the barrel section was set as from feeding section 135°C to discharge end as 175°C. The rotor speed was set as 600 rpm. The discharge door was opened as 50% of the fully open state. The feeding rate and ultrasonic power were set according to Table I. The extrudate was collected and compressed to round pie while hot, and then numbered in order from the beginning to the end of processing. The samples numbered in the middle rearward were crushed into pellets for compression molding or injection molding.

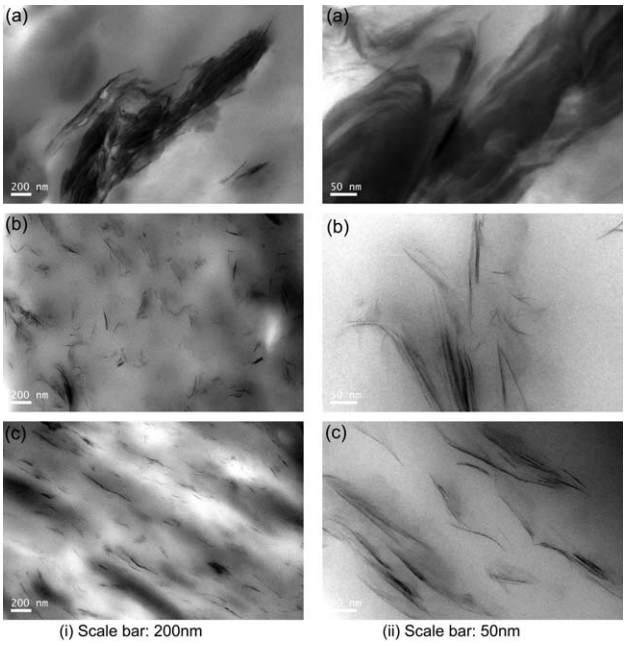

Figure 3. TEM micrographs of PP nanocomposites containing 0 ph PP-*g*-MA without ultrasonic treatment (a), 15 ph PP-*g*-MA without (b) and with (c) ultrasonic treatment at a power of 810 W.

Prepared nanocomposites were compression molded into discs of 25 mm diameter and 2 mm thickness at 180°C using a compression molding press (YT-LH102A, Dongguan Yitong test & technology, Dongguan, China) for the rheological measurements. The samples for X-ray diffraction (XRD) analysis were also compression molded into rectangular of 10 × 6 × 3 mm^3. Tensile bars (ASTM D-638) and notched impact bars (ASTM D-256) were prepared by injection molding.

Measurements and Characterization

The XRD experiments were performed on a Rigaku D/max 2550 VB/PC X-ray diffractometer using incident CuK_a radiation with a wavelength of 1.54 Å. The angular range of small angle XRD was from 1.2° to 10°, and the scanning speed was 1.3°/min. The basal spacing of OMMT was estimated from the (001) diffraction. The angular range of wide angle X-ray diffraction (WAXD) was from 3° to 50°, and the scanning speed was 6°/min.

Transmission electron microscopy (TEM) analysis of the nanocomposites was carried out with Tecnai G2 Spirit Biotwin TEM, which was operated at an accelerating voltage of 120 kV. Ultra thin specimens (100 nm) were cut from the middle section of the injection molded specimens. Cutting operations were carried out under cryogenic conditions with a microtome (Leica Ultracut UCT) at −80°C.

Scanning electron microscopy (SEM) images were obtained with a Hitachi S-4800 SEM, operating at an accelerating voltage of 5 kV. Samples were cryofractured from injection molded specimens and the rubbery phase (SEBS) was extracted with heptane to observe the morphology of the cavities that correspond to the volume initially occupied by this phase. SEM micrographs were analyzed by ImageJ 1.41 to determine the diameter of each cavity. Four hundred cavities in each micrograph were selected for statistic; the cavity size distribution was shown by the statistical histogram. The number average

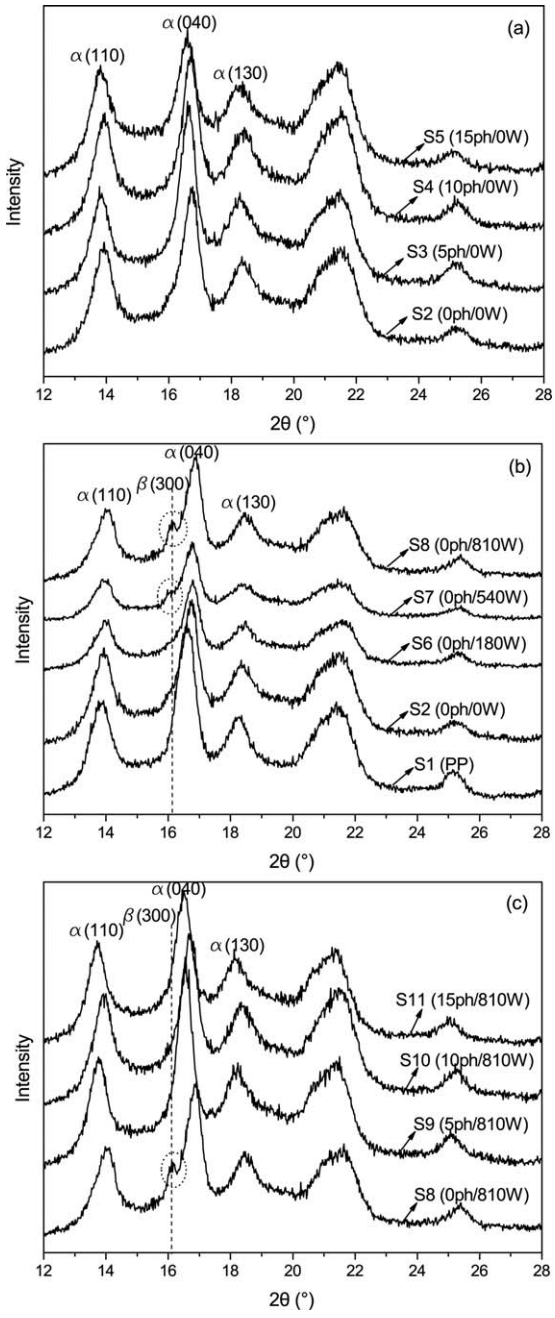

Figure 4. Wide-angle XRD patterns of neat PP and its nanocomposites at different amounts of compatibilizer without ultrasonic treatment (a) and at different ultrasonic powers without compatibilizer (b), as well as the patterns of samples with both compatibilizer and ultrasonic treatment at a power of 810 W (c).

diameter (d_n) and weight average diameter (d_w) were calculated according to the following formula[26]:

$$d_n = \frac{\sum_{i=1}^{N} n_i d_i}{\sum_{i=1}^{N} n_i} \quad (1)$$

$$d_w = \frac{\sum_{i=1}^{N} n_i d_i^2}{\sum_{i=1}^{N} n_i d_i} \quad (2)$$

where n_i and d_i are the number and the diameter of the ith particle, respectively.

The rheological properties were measured using Bohlin Gemini 2 by Malvern Instruments with a dynamic mode frequency sweep process at 190°C. Parallel plate with a diameter of 25 mm and a gap size of 1 mm was used. Complex viscosity, storage and loss modulus as a function of angular frequency ranging from 0.01 to 100 rad/s were measured. A fixed strain of 5% was used to ensure that measurements were carried out within the linear viscoelastic range of the materials investigated.

According to ASTM D-638, tensile properties were tested with RGM-2020 Universal Testing Machine (Shenzhen Reger Instrument, Shenzhen, China) at a testing speed of 50mm/min. According to ASTM D-256, notched impact strength was measured using PTM1100-B1 Impact-Testing Machine (SUNS, Shenzhen, China). At least five samples of each experiment were tested. All the tests were carried out at room temperature.

RESULTS AND DISCUSSION

Structural Effects

The small-angle XRD patterns of OMMT and PP/SEBS/OMMT nanocomposites at different PP-*g*-MA loadings without [Figure 2(a)] and with [Figure 2(b)] ultrasonic treatment is shown in Figure 2. The basal distances are calculated by Bragg's law ($n\lambda = 2d \sin\theta$). As we can see in Figure 2, the (001) plane peaks of nanocomposites were shifted to lower angles in comparison with DK1N, showing that the interlayer distances were enlarged. This indicates that PP and SEBS chains had intercalated into the interlayers of DK1N. As shown in Figure 2(a), the basal spacing increased with increased PP-*g*-MA concentration. When the PP-*g*-MA concentration increased to 15ph, this peak disappeared, indicating an exfoliation of OMMT by PP matrix. At the same time, the more significant increase in interlayer distance was observed in PP nanocomposites with ultrasonic treatment at an power of 810 W [Figure 2(b)]. The

Table II. Integrated Area of the Diffraction Peaks, Relative Amount of β-form PP (K) of PP Nanocomposites

Sample	S2	S3	S4	S5	S6	S7	S8	S9	S10	S11
A_{110}	23,940	20,403	25,324	22,293	15,179	13,027	18,506	20,987	21,658	18,435
A_{300} (A_β)	/	/	/	/	/	2836	4041	/	/	/
A_{040}	28,370	32,048	29,580	20,584	23,936	22,196	24,926	32,481	27,164	24,761
A_{130}	11,195	10,419	13,617	9007	8567	7476	8934	10,333	11,464	10,108
K	/	/	/	/	/	0.0623	0.0716	/	/	/

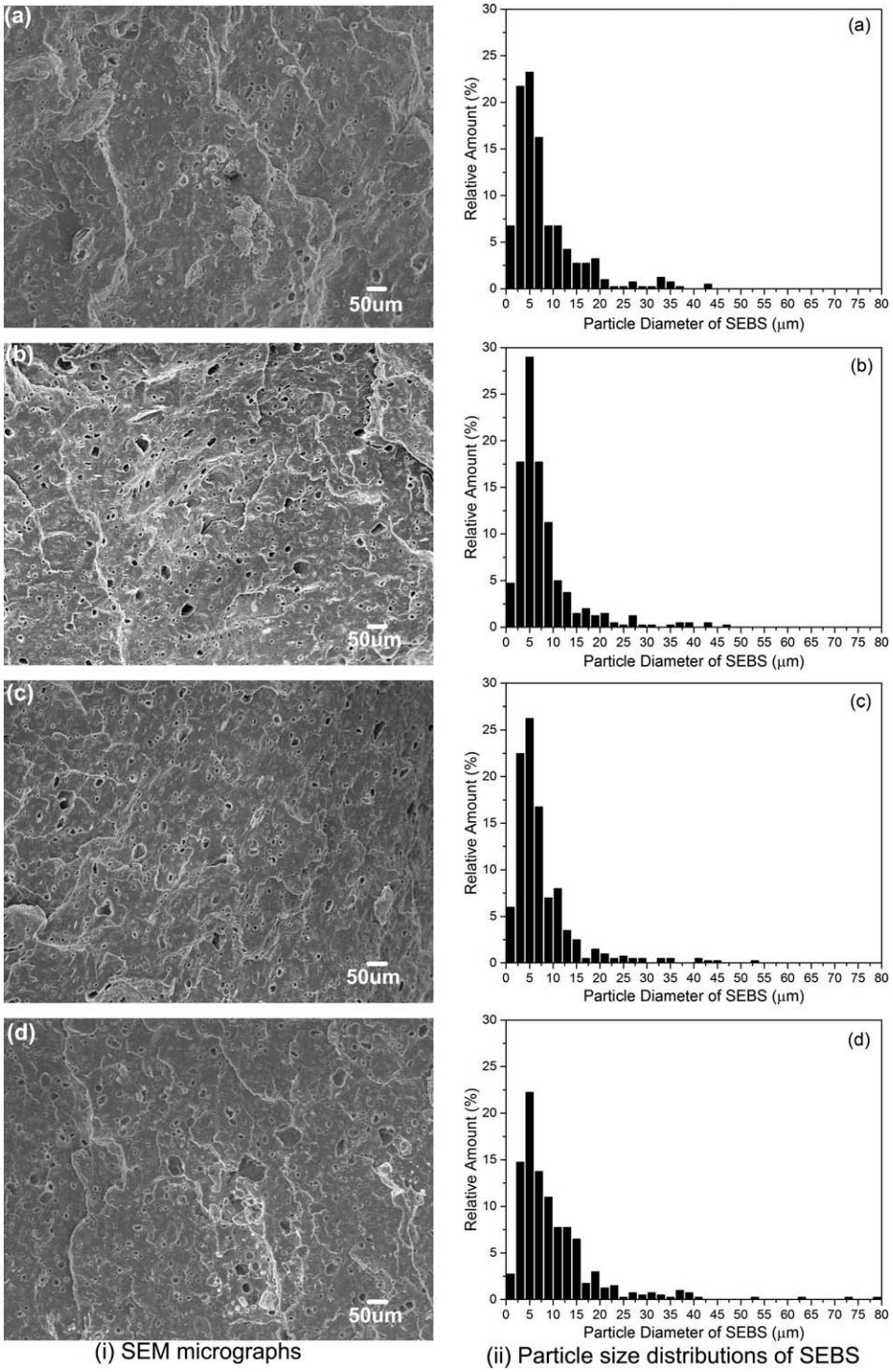

Figure 5. SEM micrographs (i) of cryofractured sample surface and particle size distributions (ii) of SEBS in PP nanocomposites without ultrasonic treatment at a feeding rate of 3.5 kg/h (a, S2) and with ultrasonic treatment of 810 W at different feeding rates: 3.5 kg/h (b, S8), 1.5 kg/h (c, S12), and 5.5 kg/h (d, S15).

d-spacing of ultrasonically treated nanocomposites was more than that of untreated samples at the same PP-*g*-MA loading. Moreover, the clay was ultrasonically exfoliated by adding only 10 ph compatibilizer. Apparently, the nanocomposites with exfoliated OMMT can be prepared with incorporation of less compatibilizer when assisted by ultrasound.

The intercalation and exfoliation of the clay in the system can be further supported by TEM analysis; the results are demonstrated in Figure 3. Figure 3(a) shows TEM micrographs of PP/SEBS/OMMT nanocomposite, which was neither compatibilized by PP-*g*-MA nor treated by ultrasound. It was observed that the clay is not well dispersed in the system individual tactoids of

Table III. Average Diameter of SEBS in PP Nanocomposites

Sample	Ultrasonic power (W)	Feeding rate (kg/h)	d_n (μm)	d_w (μm)
S2	0	3.5	8.17	14.18
S8	810	3.5	7.75	13.75
S12	810	1.5	7.39	14.03
S15	810	5.5	10.04	18.8

the layered clays are visible. The addition of PP-*g*-MA could enhance the dispersion of OMMT tactoids throughout the system [compared to the sample without PP-*g*-MA, as shown in Figure 3(a)], the mainly intercalated and partially exfoliated clays were found in Figure 3(b). The OMMT tactoids could be further disrupted by high power ultrasound, showing that more nanoclays were exfoliated and uniformly distributed in the system, as shown in Figure 3(c). In addition, it was found that the ultrasonic irradiation could induce orientation of the layered clays in the system.

Figure 4 shows the wide-angle XRD patterns of neat PP and its nanocomposites at different amounts of compatibilizer without ultrasonic treatment [Figure 4(a)] and at different ultrasonic powers without compatibilizer [Figure 4(b)], as well as the patterns of samples with both compatibilizer and ultrasonic treatment at a power of 810W [Figure 4(c)]. It is well known that isotactic polypropylene (iPP) has α, β, γ, δ and smectic forms. Among these crystal structures, the α-form PP, which exhibits great brittleness, holds a strong majority in iPP. However, the β-form PP, demonstrating a higher impact toughness, almost can not be found in neat iPP. As shown in Figure 4(a), the diffraction peaks of α-form PP, corresponding to (110), (040), and (130) planes, are observed, while the diffraction peak of β-form PP which corresponds to (300) plane cannot be found. This shows that the crystal structures of iPP cannot be affected by PP-*g*-MA. When the composites were treated by ultrasound at a power of 540 W without adding PP-*g*-MA [Figure 4(b)], a weak diffraction peak of (300) plane appeared. As the ultrasonic power increased to 810 W, this peak could be obviously observed. However, the diffraction peak of (300) plane disappeared when PP-*g*-MA was incorporated [Figure 4(c)], even though the composites were treated by ultrasound. Therefore, we can conclude that the formation of β-form PP can be induced by ultrasonic irradiation with higher intensity, whereas it would be suppressed by PP-*g*-MA. This might be owing to several factors such as eutectic effect of PP-*g*-MA on PP, nucleation and acidity of the carboxyl group of PP-*g*-MA.[27]

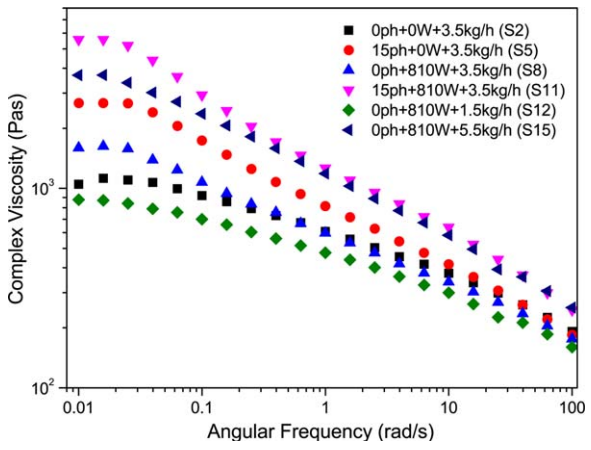

Figure 6. Complex viscosity of PP/SEBS/OMMT nanocomposites as a function of angular frequency. [Color figure can be viewed in the online issue, which is available at wileyonlinelibrary.com.]

The relative amount of β-form PP in iPP is represented by K value, which can be calculated according to the following formula[12]:

$$K = \frac{A_\beta}{A_{110} + A_{040} + A_{130} + A_\beta} \quad (3)$$

where A_β is the integrated area of the (300) diffraction peak of β-form PP, A_{110}, A_{040}, and A_{130} are the integrated area of (110), (040), and (130) diffraction peaks of α-form PP, respectively. The integrated area of the diffraction peaks and K value of PP nanocomposites are listed in Table II. Apparently, the ultrasonic oscillation can induce the formation of β-form PP, whose relative-amount are 6.23 and 7.16% which correspond to the ultrasonic power of 540 and 810 W, respectively. This implies that the ultrasonic vibration can promote the polymorphic transitions of iPP from the monoclinic (α) form to the hexagonal (β) form, which agrees well with the reports by Cao et al.[28,29]

As mentioned above, β-form PP could enhance the impact toughness of PP nanocomposites. Figure 9(a) shows the impact strength of samples treated and untreated by ultrasound at different PP-*g*-MA concentrations. The impact strength of ultrasonically treated samples were higher than that of untreated ones. However, the impact strength of both treated and untreated samples decreased with the increase of PP-*g*-MA loadings. One possible reason is that the formation of β-form PP can be induced by ultrasound and can be suppressed by PP-*g*-MA.

SEM Analysis

As well known, the dispersion of elastomer in PP matrix plays an important role in the toughening effect of PP. Figure 5 shows the SEM micrographs of cryofractured sample surface and the statistical histograms of particle size distributions of SEBS in PP nanocomposites without and with ultrasonic treatment of 810 W at different feeding rates. The rubbery phase (SEBS) was extracted with heptane, so the morphology of the cavities correspond to the volume initially occupied by SEBS. As can be seen in Figure 5, SEBS particles are much finer and denser in PP/SEBS/OMMT system with ultrasonic irradiation [Figure 5(b)] than in that without ultrasonic treatment [Figure 5(a)] at the same feeding rate of 3.5 kg/h. Likewise, SEBS are more uniformly distributed across the whole matrix treated by ultrasound. Furthermore, the particle size of SEBS decreased with the decrease of feeding rate, indicating that a longer residence time of ultrasonic treatment could improve the dispersion of SEBS in PP nanocomposites.

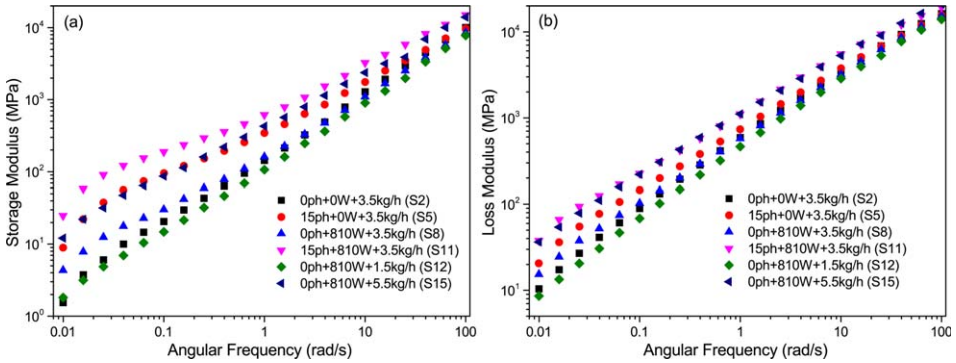

Figure 7. Storage (a) and loss (b) modulus of PP/SEBS/OMMT nanocomposites as a function of angular frequency. [Color figure can be viewed in the online issue, which is available at wileyonlinelibrary.com.]

The enhanced dispersion can also be described by statistical histograms of particle size distributions shown in Figure 5. The particle size distributions of SEBS in PP nanocomposites treated by ultrasound are narrower than that of samples without ultrasonic treatment. The relative amount of SEBS particles with particle diameters of 0–10 μm increased from 53.5 to 71.5% with a decrease from 5.5 to 1.5 kg/h in feeding rate respectively. The average particle size including the number average particle diameter (d_n) and weight average particle diameter (d_w) obtained from SEM analysis, are listed in Table III. It was found that d_n and d_w of SEBS in ultrasonically treated system (S8) were less than those in untreated system (S2). Moreover, the two average diameters of SEBS in ultrasonically treated systems decreased with the decrease of feeding rate. This is because the samples prepared at lower feeding rate subject to ultrasonic irradiation at a longer residence time, so that the dispersion of SEBS can be enhanced due to the adequate ultrasonic treatment and mixing of rotors.

From the above analysis, it can be concluded that the introduction of ultrasound is beneficial to improve the dispersion of SEBS in PP nanocomposites so as to increase the impact strength which is to be discussed later.

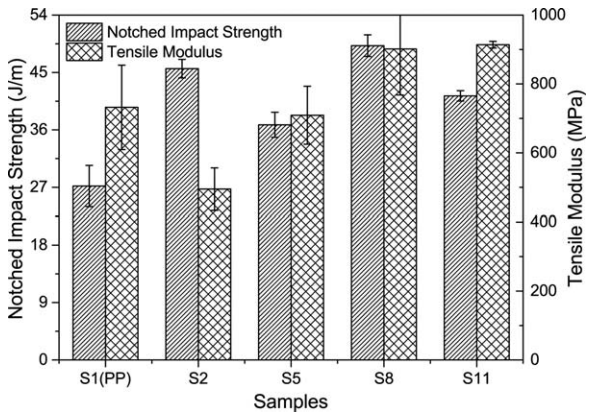

Figure 8. Mechanical properties of PP and its nanocomposites (S1: Neat PP, S2: PP/SEBS/OMMT, S5: PP/SEBS/OMMT/PP-*g*-MA, S8: PP/SEBS/OMMT/Ultrasound, S11: PP/SEBS/OMMT/PP-*g*-MA/Ultrasound).

Rheology

The effects of PP-*g*-MA and ultrasound on the complex viscosity of nanocomposites as a function of angular frequency at the same SEBS and OMMT content are shown in Figure 6. It was found that the complex viscosity of nanocomposites increased with increasing PP-*g*-MA concentration. Moreover, the complex viscosity increased further with ultrasonic treatment. The great enhancement of complex viscosities of nanocomposites with incorporation of PP-*g*-MA and ultrasonic treatment was attributed to the mainly intercalated and partially exfoliated silicate layers in nanocomposites, which can be observed from XRD results and TEM micrographs as discussed above. Besides, the viscosity decreased with the decrease of feeding rate, which might be owing to increasing polymer degradation at longer residence time in the treatment zone.[21] As Li[30] reported, ultrasonic irradiation with higher intensity could cause a random scission of polymer chains that is the degradation of polymer melt. The degradation extent strongly depends on the time of irradiation. Since the degradation lowers the molecular weight of polymer, it directly weakens the intermolecular interaction between molecular chains. Therefore, the viscosity decreased when the composites suffered ultrasonic irradiation at longer residence time.

The enhanced dispersion of OMMT can be further verified by the increase in storage modulus and loss modulus of PP nanocomposites, as shown in Figure 7. The two modulus of nanocomposites containing PP-*g*-MA were higher than those without compatibilizer and could be further increased by ultrasonic treatment. However, both modulus decreased with decreasing feeding rate, which was also due to the polymer degradation at a longer time of ultrasonic treatment. All of these results indicated that PP-*g*-MA, as a compatibilizer between PP and OMMT, could directly improve the compatibilization, which was good for the intercalation of molecular chains of PP and SEBS. Moreover, the OMMT, in the form of fragments, could be crushed into the intercalated or exfoliated layers by ultrasonic vibration. Therefore, the improved dispersion of OMMT in PP nanocomposites with enhanced polymer-OMMT interaction leads to an increase of their viscosity and a reduction in the mobility of the polymer chains.

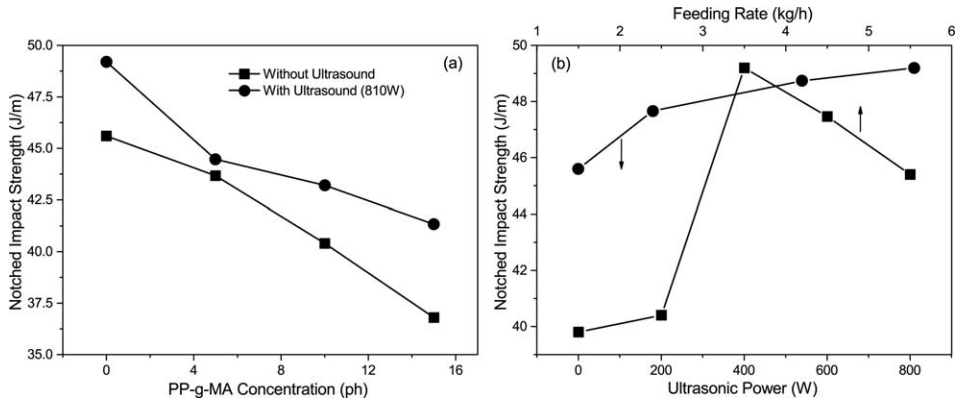

Figure 9. Notched impact strength as a function of PP-*g*-MA concentration (a), ultrasonic power and feeding rate (b).

Mechanical Properties

The mechanical properties, including notched impact strength, tensile strength and tensile modulus of PP and all the nanocomposites prepared in this research have been drawn in Figures 8–11. It can be observed in Figure 8 that the addition of SEBS into PP leads to a great increase of impact strength, but a decrease of tensile modulus of S2 compared with neat PP (S1). As the PP-*g*-MA was added (S5, S11) or the composites were treated by ultrasound (S8, S11), the tensile modulus of PP nanocomposites was enhanced. The increased tensile modulus could indicate a higher stiffness, which was attributed to the enhanced dispersion of OMMT in PP matrix with the help of ultrasonic irradiation and the improved compatibility between PP and OMMT. Furthermore, the impact strength and tensile strength of ultrasonically treated samples were higher than that of the untreated ones at the same PP-*g*-MA loading. However, the impact strength decreased when PP-*g*-MA was incorporated, and the detailed explanations are to be discussed later.

Figure 9 shows the notched impact strength of PP nanocomposites under different PP-*g*-MA concentrations and ultrasonic intensities. The impact strength [Figure 9(a)] decreased with the increase of PP-*g*-MA concentration, indicating that the incorporation of PP-*g*-MA cannot benefit the toughening for PP, which agrees well with the report by Su and Huang.[13] This might be attributed to the intrinsic mechanical properties of commercial PP-*g*-MA.[13] Another possible reason is that the increase in PP-*g*-MA concentration is equivalent to the relative decrease in the percent content of SEBS. Besides, the toughness of ultrasonically treated samples was better than that of untreated ones at the same PP-*g*-MA content. From Figure 9(b), the impact strength of samples increased with the increase of ultrasonic intensity including ultrasonic power and ultrasonic time (feeding rate). The toughness of nanocomposites can be enhanced by ultrasonic treatment for several reasons: (1) Ultrasonic oscillations can break up large agglomerates of SEBS into finer particles, leading to an improved dispersion in PP matrix and the interfacial adhesion. This can also be substantiated by the decrease in particle diameters of SEBS through SEM analysis as shown above; (2) According to the previous XRD analysis, ultrasound with certain intensity can induce the growth of β-form PP which demonstrates the higher impact strength; (3) The long chain molecules of PP and SEBS can be scissored into macroradicals by ultrasonic oscillations. The macroradicals react with each other, generating block or graft copolymers,[31] which can be taken as a compatibilizer to achieve *in situ* compatibilization between PP and SEBS. However, it was found that the impact strength began to decrease when the feeding rate reached 3.5 kg/h. This may be due to inadequate treatment of ultrasound at a higher feeding rate. At the same time, a sharp decrease of impact strength was observed at a lower feeding rate. This may be explained by the

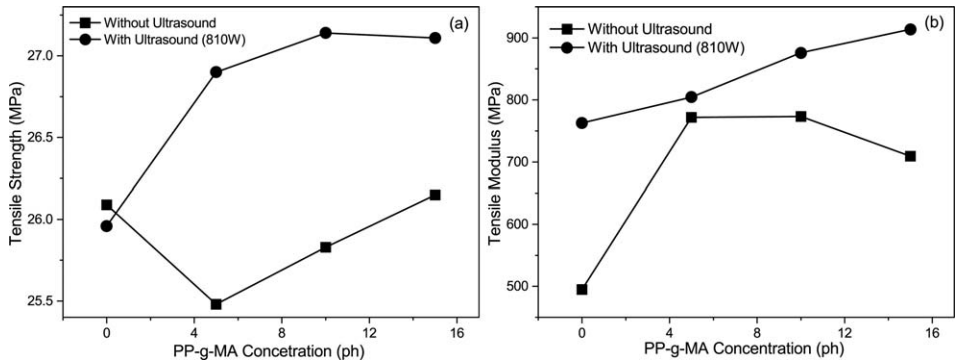

Figure 10. Tensile strength (a) and tensile modulus (b) as a function of PP-*g*-MA concentration with and without ultrasonic treatment.

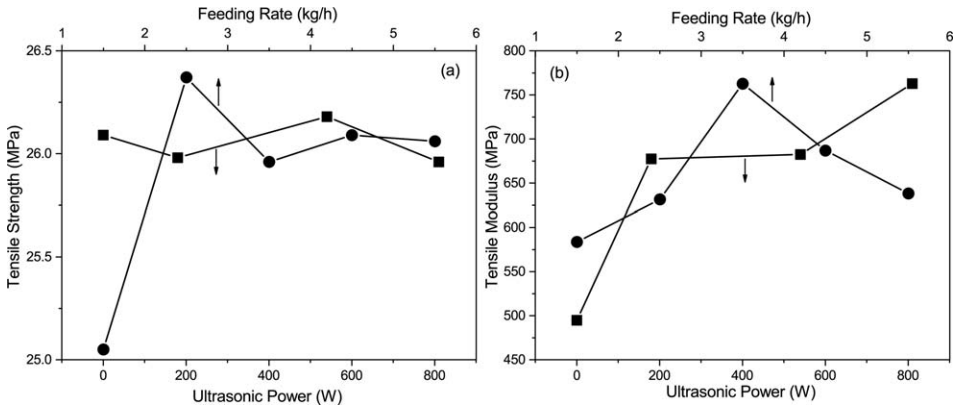

Figure 11. Tensile strength (a) and tensile modulus (b) as a function of ultrasonic power and feeding rate.

polymer degradation when the polymer melt subjects ultrasonic treatment for a longer time.

The effect of compatibilizer on the tensile strength and tensile modulus of ultrasonically treated and untreated nanocomposites is shown in Figure 10. There is an increase in tensile strength and tensile modulus of nanocomposites with an increase in PP-*g*-MA loadings. It is worth noting that the strength and stiffness of ultrasonically treated samples are enhanced in comparison with the untreated ones at the same PP-*g*-MA concentration. More details about the effect of ultrasound on tensile strength and tensile modulus of nanocomposites are illustrated in Figure 11. The tensile strength of samples was little changed with an increase in ultrasonic power and feeding rate [Figure 11(a)]. From Figure 11(b), the tensile modulus of samples increased with increasing ultrasonic power whereas the tensile modulus of samples increased to 763 MPa at a feeding rate of 3.5 kg/h and then decreased to 638 MPa at 5.5 kg/h.

Therefore, from the results of mechanical properties, it was concluded that ultrasound could enhance the dispersion of OMMT and SEBS in PP by creating strong interfacial adhesion of clay and SEBS with the matrix, but ultrasound with higher intensity may result in polymer degradation, which is bad for the mechanical properties. In addition, OMMT could be well dispersed in PP by incorporation of PP-*g*-MA so as to improve the stiffness of PP nanocomposites. However, the toughness might be reduced by the increasing PP-*g*-MA. Thus, it is believed that the synergistic effect of both ultrasound and compatibilizer should account for the balance between toughness and stiffness of PP/SEBS/OMMT ternary nanocomposites.

CONCLUSIONS

To obtain a uniform dispersion of OMMT and SEBS in PP matrix and to achieve a right balance between stiffness and toughness of PP/SEBS/OMMT ternary nanocomposites, effects of PP-*g*-MA and ultrasound on structural, rheological, and mechanical properties of PP nanocomposites were studied. The results showed that addition of PP-*g*-MA could improve the compatibility between PP and OMMT, and then achieved a rapid intercalation and a partial exfoliation of PP/SEBS/OMMT nanocomposite. Moreover, it has been proved that ultrasonic oscillation could help to break up the agglomerates of OMMT and SEBS in PP matrix, leading to the increase of *d*-spacing, complex viscosity and mechanical properties. The impact strength and tensile modulus of ultrasonically treated samples were higher than those of untreated ones. In addition, the impact strength and tensile modulus increased with the increase of ultrasonic intensity. However, the incorporation of PP-*g*-MA would reduce the impact strength of PP nanocomposites. Besides, the mechanical properties would be weakened due to the polymer degradation caused by ultrasonic irradiation for a longer residence time. Therefore, it is believed that the synergistic effect of both compatibilizer and ultrasound should account for the balance between toughness and stiffness of PP/SEBS/OMMT ternary nanocomposites.

ACKNOWLEDGMENTS

The authors sincerely acknowledge the National Natural Science Foundation of China (Grant No. 51273065).

REFERENCES

1. Bao, S. P.; Tjong, S. C. *Compos. A*, **2007**, *38*, 378.
2. Tjong, S. C.; Xu, S. A.; Li, R. K.-Y.; Mai, Y. W. *Compos. Sci. Technol.* **2002**, *62*, 831.
3. Denac, M.; Musil, V.; Šmit, I. *Compos. A* **2005**, *36*, 1282.
4. Ma, C. G.; Mai, Y. L.; Rong, M. Z.; Ruan, W. H.; Zhang, M. Q. *Compos. Sci. Technol.* **2007**, *67*, 2997.
5. Bendjaouahdou, C.; Bensaad, S. *Energy Proc.* **2013**, *36*, 574.
6. Hikasa, S.; Nagata, K.; Nakamura, Y. *J. Adhes. Sci. Technol.* **2011**, *25*, 2615.
7. Hejazi, I.; Sharif, F.; Garmabi, H. *Mater. Des.* **2011**, *32*, 3803.
8. Lee, H.; Fasulo, P. D.; Rodgers, W. R.; Paul, D. R. *Polymer* **2005**, *46*, 11673.
9. Liu, Y.; Kontopoulou, M. *Polymer* **2006**, *47*, 7731.
10. Martins, C. G.; Larocca, N. M.; Paul, D. R.; Pessan, L. A. *Polymer* **2009**, *50*, 1743.
11. Su, F. H.; Huang, H. X.; Zhao, Y. *Compos. B* **2011**, *42*, 421.
12. Tjong, S. C.; Bao, S. P.; Liang, G. D. *J. Polym. Sci. Part B: Polym. Phys.* **2005**, *43*, 3112.

13. Su, F. H.; Huang, H. X. *J. Appl. Polym. Sci.* **2009**, *112*, 3016.
14. Vuluga, Z.; Panaitescu, D. M.; Radovici, C.; Nicolae, C.; Iorga, M. D. *Polym. Bull.* **2012**, *69*, 1073.
15. Tan, X. M.; Xu, Y. S.; Cai, N.; Jia, G. W. *Polym. Compos.* **2009**, *30*, 835.
16. Swain, S. K.; Isayev, A. I. *Polymer* **2007**, *48*, 281.
17. Ryu, J. G.; Kim, H.; Lee, J. W. *Polym. Eng. Sci.* **2004**, *44*, 1198.
18. Isayev, A. I.; Kumar, R.; Lewis, T. M. *Polymer* **2009**, *50*, 250.
19. Horrocks, A. R.; Kandola, B.; Milnes, G. J.; Sitpalan, A.; Hadimani, R. L. *Polym. Degrad. Stab.* **2012**, *97*, 2511.
20. Lee, E. C.; Mielewski, D. F.; Baird, R. *J. Polym. Eng. Sci.* **2004**, *44*, 1773.
21. Lapshin, S.; Isayev, A. I. *J. Vinyl Addit. Technol.* **2006**, *12*, 78.
22. Kim, K. Y.; Nam, G. J.; Lee, J. W. *Compos. Interfaces* **2007**, *14*, 533.
23. Wang, X.; Pang, S. L.; Yang, J. H.; Yang, F. *Trans. Nonferrous Metals Soc. China* **2006**, *16*, s524.
24. Liu, S. P.; Liang, C. W. *Int. Commun. Heat Mass Trans.* **2011**, *38*, 434.
25. Martin, Z.; Jimenez, I.; Gomez, M. A.; Ade, H.; Kilcoyne, D. A. *Macromolecules* **2010**, *43*, 448.
26. Premphet, K.; Paecharoenchai, W. *J. Appl. Polym. Sci.* **2001**, *82*, 2140.
27. Yuan, X. L.; Zhang, Y. X.; Zhang, X. F. *Polym. Mater. Sci. Eng.* **1999**, *15*, 112 (in Chinese).
28. Cao, Y. R.; Li, H. L. *Polym. Eng. Sci.* **2002**, *42*, 1534.
29. Cao, Y. R.; Xiang, M.; Li, H. L. *J. Appl. Polym. Sci.* **2002**, *84*, 1956.
30. Li, Y.; Li, J.; Guo, S.; Li, H. *Ultrason. Sonochem.* **2005**, *12*, 183.
31. Oh, J. S.; Isayev, A. I.; Rogunova, M. A. *Polymer* **2003**, *44*, 2337.